Chemical Physics xxx (2012) xxx–xxx

Contents lists available at SciVerse ScienceDirect

Chemical Physics

journal homepage: www.elsevier.com/locate/chemphys

Orientation distribution function and order parameters of oriented spin probe as determined by EPR spectroscopy

Andrey Kh. Vorobiev *, Tatiana S. Yankova, Natalia A. Chumakova

Department of Chemistry, M.V. Lomonosov Moscow State University, 119992 Moscow, Leninskie Gory, Russia

ARTICLE INFO

Article history:
Received 28 June 2012
In final form 16 October 2012
Available online xxxx

Keywords:
Electron paramagnetic resonance
Molecular orientational order
Orientation distribution function
Order parameters
Spectra simulation

ABSTRACT

Two methods for determination of molecular orientation distribution from angular dependence of EPR spectra are compared. One of these methods is based on direct expansion of the orientation distribution function in a series of generalized spherical harmonics, in another method the mean field potential is used. The limitations of these approaches as well as their capabilities and advantages are considered

1. Introduction

It is well known that molecular orientational alignment is an important feature of liquid crystals, oriented polymers, biopolymers and other materials. The most comprehensive description of molecular orientational order is an orientation distribution function (ODF) $\rho(\alpha,\beta,\gamma)$, where α, β, γ are Euler angles defining the relative orientation of the molecular reference frame and the sample frame. ODF gives the probability density of particles orientation with angles α, β, γ, so that $dN = \rho(\alpha,\beta,\gamma)sin\beta d\alpha d\beta d\gamma$. The orientation distribution function can be presented as an expansion in a series of generalized spherical harmonics (elements of Wigner D-matrix):

$$\rho(\alpha,\beta,\gamma) = \sum_{j,m',m} \frac{2j+1}{8\pi^2} \left\langle D^j_{m'm}{}^* \right\rangle D^j_{m'm}(\alpha,\beta,\gamma) \tag{1}$$

In case of uniaxial sample the series Eq. (1) can be simplified using Legendre polynomials $P_j(\cos\beta)$ and associated Legendre polynomials $P_{jm}(\cos\beta)$:

$$\rho(\beta,\gamma) = \frac{1}{2\pi}\sum_{j=0}^{\infty}\left(\frac{1}{2}a_{j0}P_j(\cos\beta) + \sum_{m=1}^{j} P_{jm}(\cos\beta)\left[a_{jm}\cos m\gamma + b_{jm}\sin m\gamma\right]\right) \tag{2}$$

The expansion coefficients $\langle D^j_{m'm}{}^* \rangle$ (or a_{jm}, b_{jm}) provide a set of order parameters. The concept of order parameters is considered in detail in [1]. To characterize order parameters of uniaxial system in real numbers the following expressions are used:

$$\begin{aligned} A^j_m &\equiv S_{jm} = \frac{\langle D^j_{0m}{}^* \rangle + \langle D^j_{0-m}{}^* \rangle}{2} = \frac{a_{jm}}{2j+1}\sqrt{\frac{(j+m)!}{(j-m)!}} \\ B^j_m &= \frac{\langle D^j_{0m}{}^* \rangle + \langle D^j_{0-m}{}^* \rangle}{2i} = \frac{b_{jm}}{2j+1}\sqrt{\frac{(j+m)!}{(j-m)!}} \end{aligned} \tag{2a}$$

Orientational order can be described using orientation factors and elements of Saupe orientation matrix as well. Different sets of orientation characteristics are convenient for description of different systems and experiments. However, all these characteristics can be easily transformed from one form to another one. The brief comparison of the orientation characteristics is presented, for example, in [2].

Specification of all order parameters gives a complete specification of orientation distribution function. Unfortunately, at present time there is no technique available for complete experimental determination of orientation distribution function for soft matter. Only second moments of ODF (order parameters of rank 2) are determined usually since they can be obtained using one-photon optical methods. The orientation characteristics of rank 4 are determined experimentally rather rarely. EPR spectroscopy combined with spin probe and spin label techniques provides, in principle, the possibility of more complete determination of an orientation distribution function. This aim can be achieved by numerical simulation of EPR spectra, recorded at different orientations of examined sample in magnetic field of the spectrometer. Obvious limitation of this technique is the symmetry of the spin Hamiltonian with respect to inversion of coordinate system. It means that EPR spectra recorded at direct and opposite directions of magnetic field are quite the same. As a result of this feature even order parameters (coefficients of expansion Eq. (1)) can be determined only. Other limitations, imposed on extractable characteristics of orientational

* Corresponding author.
E-mail address: a.kh.vorobiev@gmail.com (A.Kh. Vorobiev).

0301-0104/$ - see front matter © 2012 Elsevier B.V. All rights reserved.
http://dx.doi.org/10.1016/j.chemphys.2012.10.006

distribution by symmetry of sample, probe molecule and spin Hamiltonian are considered in details elsewhere [2,3].

The most widespread method of simulation of EPR spectra with determination of orientation distribution function is the method, described in [4–6]. In this approach the orientational order of spin probe (or label) is described using mean force approximation. The molecular orientational alignment is considered as a result of action of mean field potential $U(\alpha,\beta,\gamma)$ at the conditions of Boltzmann equilibrium as follows:

$$\rho(\beta,\gamma)=\frac{e^{-U(\beta,\gamma)/k_bT}}{\int e^{-U(\beta,\gamma)/k_bT}\sin\beta d\beta d\gamma} \tag{3}$$

where the orienting potential is expanded in a series of spherical Wigner D-functions:

$$\frac{U(\beta,\gamma)}{k_bT}=-\sum_{j,m}c_{jm}D^{j}_{0m}(\beta,\gamma) \tag{4}$$

Eq. (4) is used commonly in the following form:

$$\frac{U(\beta,\gamma)}{k_bT}=-\sum_{j}c_{j0}D^{j}_{00}(\beta,\gamma)-\sum_{j,m}c_{jm}\left[D^{j}_{0m}(\beta,\gamma)+D^{j}_{0-m}(\beta,\gamma)\right] \tag{4a}$$

where j, $m = 2, 4$.

This approach was developed in the 1970s (see, for example, [7]). There is extensive literature, describing applications of this approach. In the earlier works the parameters of ODF were determined by means of trial-and-error way [8–10]. Now the nonlinear least-squares minimization of discrepancies between calculated and experimental spectra is used [11,12]. The different fitting algorithms are considered in [13]. The most widespread software realization of the approach is described in [4–6]. The program is based on the stochastic Liouville equation (SLE) and, thus, it is intended for calculation of EPR spectra of rotating particles. The similar method is incorporated in integrated software *E-SpiReS* aimed at interpretation of EPR spectra in fluids [14,15]. A lot of useful and interesting results were obtained using this approach with available software. This model will below be referred to as OP (orienting potential) approach. An alternative approach is based on determination of an orientation distribution function immediately in form of Eq. (1) or Eq. (2) (OD approach) [16–21]. Comparison of these two approaches and determination of their applicability are subjects of this contribution.

2. Qualitative consideration

The reference frames used are shown in Fig. 1. Sample frame (SF) is associated with the macroscopic director of oriented medium. At every point of the oriented medium there is local orientational alignment with local main direction fixed with local frame (LF). The paramagnetic molecule, located in the medium, is characterized by molecular orientation axes, which form the molecular orientation frame (MOF). Tensor of rotational diffusion, g-tensor and hfi-tensor are diagonal in their own molecular frames RF, gF, AF accordingly. The set of Euler angles that transforms one frame to another one is designated by Ω.

2.1. Some features of OP and OD approaches

1. In accordance with OP let us assume, that the local director in all points of the medium coincides with macroscopic sample director ($\Omega_{SF\to MOF}\equiv\Omega_{LF\to MOF}\equiv\Omega$), and orientational order of paramagnetic molecules is induced by the orienting potential (Eq. (3)) at the temperature T_0:

$$\rho_o(\Omega)=\frac{1}{N}e^{-U(\Omega)/k_bT_0} \tag{5}$$

where $N=\int e^{-U(\Omega)/k_bT}d\Omega$ is normalization factor.

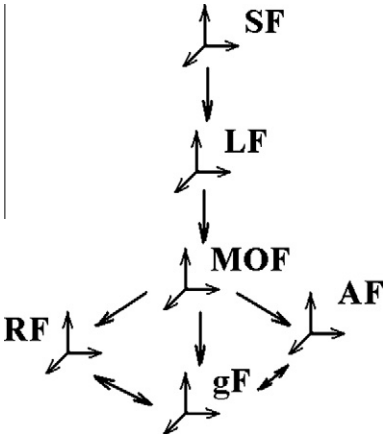

Fig. 1. Reference frames used in the text.

When the temperature of the sample is changed, the relaxation processes, directed to the new Boltzmann equilibrium, take place. The evolution of the orientation distribution function can be presented as:

$$\rho(t)=\frac{1}{N}[\rho_1+((\rho_0-\rho_1)f(t)] \tag{6}$$

where ρ_1 is the equilibrium orientation distribution function at new temperature T_1; function $f(t)$ describes kinetics of relaxation.

In the simplest case $f(t)$ is the exponential decay function. In general case relaxation kinetics is defined by one or more characteristic times τ. Taking into account the anisotropy of rotation we should conclude, that characteristic time is angular dependent:

$$f(t)=f\left[\frac{t}{\tau(\Omega)}\right]\equiv\xi(t,\Omega) \tag{7}$$

If the cooling of the sample is sufficiently rapid and deep, the overcooled glassy state is achieved, where the relaxation is not finished within the time of experiment t_{exp}. It means, that $f(t_{exp})=\xi(t_{exp},\Omega)\neq 0$. In this case the orientation distribution function state is as follows:

$$N\rho(\Omega)=\exp\left(-\frac{U(\Omega)}{k_bT_1}\right)+\left[\exp\left(-\frac{U(\Omega)}{k_bT_0}\right)-\exp\left(-\frac{U(\Omega)}{k_bT_1}\right)\right]\xi(t_{exp},\Omega) \tag{8}$$

One can see, that the orientation distribution function (Eq. (8)) does not meet the Boltzmann form (Eq. (3)). Thus, the non-equilibrium glassy state cannot be described using the OP approach.

2. The local director in general does not coincide with the sample director. It is known, that liquid crystals, membranes and other partially oriented systems often have domain structure. The orientation distribution of a sample, consisting of two domains with slightly different directors, should be described as a sum of two Boltzmann exponents. When the poly-domain sample is studied, the orientation distribution is expressed as a sum of molecular orientation distributions over all domains. It is evident, that molecular orientation in a poly-domain sample cannot be described in the framework of the distribution (3, 4) solely. The additional distribution function for domain directors is necessary. Particular case of the random local director distribution is known as MOMD model (Microscopic Order Macroscopic Disorder) [4–6]. Other examples of *a priori* assumed director distributions are described in [8,22].

The presented consideration shows, that approach (3, 4) is not valid, when the molecular orientational equilibrium has not been reached. It is rather trivial statement, but we underline it here, as the orientational degree of freedom is a very specific one. For

example, polycrystalline materials are practically in equilibrium, when other degrees of freedom are considered, but they remain far from molecular orientational equilibrium during unlimited time. Directed experimental efforts are necessary to obtain single crystal state, that is in orientational thermodynamic equilibrium.

Another important example of system with different sample and local directors is equilibrium cholesteric liquid crystalline material. The helical structure of cholesteric mesophase implies corresponding changing of local director of such systems. Thus, topics 1 and 2 demonstrate, that orientational equilibrium (Eq. (3)) is valid in the case of single domain, uniformly oriented and fast-relaxing systems only.

3. Specification of an orientation distribution function in the form of Eq. (3) presumes the existence of the potential energy surface $U(\beta,\gamma)$. As it is known, the orientational state of molecular ensemble is described taking into account not only potential energy, but entropy as well. Helmholtz free energy surface is considered in [1] and mentioned in [23]. Since ordinary experiments are performed at constant pressure, the Gibbs energy $\Delta G = \Delta H - T\Delta S$ is more appropriate function for characterization of the thermodynamic equilibrium. For example, in the framework of Marcus theory of electron transfer, equilibrium orientational order of solvent molecules around the ion is described by Gibbs energy surface [24].

Taking into account the entropy, the Eq. (3) should be rewritten as:

$$\rho(\Omega_{LF\to MOF}) = \frac{1}{N}\exp\left[-\frac{\Delta H(\Omega_{LF\to MOF})}{k_bT} + \frac{\Delta S(\Omega_{LF\to MOF})}{k_b}\right] \quad (9)$$

The following conclusions can be made from Eq. (9):

(i) The temperature dependence predicted by the Eq. (4) for orientation distribution function is not valid.
(ii) The minimum of angular dependence of enthalpy generally does not coincide with maximum of angular dependence of entropy. It means, that axis of predominant molecular orientation (MOF) is changed with temperature and presumably cannot coincide with the rotational axis, as it is assumed in [4–6].

We should notice, that the concept of molecular orientation axes in the case of rotating molecules is rather complicated, and it is beyond the scope of this work. Nevertheless it is clear, that using true molecular orientation axes (MOF) leads to diminishing of the number of expansion coefficients and to simplification of the ODF specification. For example, distribution of uniaxial molecules in uniaxial sample is described by $\left\langle D^j_{00}{}^* \right\rangle = A^j_0$ only when the own coordinate frame (MOF in Fig. 1) is used. In that case the parameters with nonzero lower indices are equal to zero. When another molecular frame (for example, g-tensor frame gF) is used for description of orientational order, the additional expansion coefficients become nonzero:

$$\left\langle D^j_{0m}{}^* \right\rangle_{gF} = A^j_0 D^j_{m0}(\varphi,\theta,0) \quad (10)$$

where φ, θ are Euler angles for transformation of gF to MOF, $\Omega_{gF\to MOF} \equiv (\varphi,\theta,0)$.

The similar expressions are valid for other molecular frames. In particular, for rotation molecular frame the Euler angles in Eq. (10) are $(\varphi,\theta,0) \equiv \Omega_{RF\to MOF}$.

Quite similar way of simplification is valid, when the OP approach is used. In the case of uniaxial molecules in uniaxial sample the coefficients c_{l0} in the expansion of potential (Eq. (4)) are nonzero only if the own molecular orientation frame (MOF) is considered. The additional nonzero coefficients c_{jm} appear when rotation frame (RF) does not coincide with MOF, but RF is used for description of orientation distribution. Such additional nonzero coefficients (most often, c_{22}) arise in course of the treatment of experimental spectra using the OP approach. These nonzero coefficients are often mistakenly interpreted as biaxiality of the molecular distribution [22,25,26].

Thus, the assumptions $SF \equiv LF$ and RF ≡ MOF are quite strong limitations and can lead to false conclusions.

Topics 1–3 show, that the OP approach is a physical model of orientational alignment, which has evident limits of applicability.

4. The OD approach is based on the following postulates:

(i) The orientation distribution of molecules exists.
(ii) The molecular orientation distribution can be described by orientation distribution function.
(iii) The orientation distribution function can be expanded in a series of orthonormal functions.
(iv) Coefficients of the series can be obtained from experimental data, in particular, from EPR spectra.

One can see that the OD approach does not use any physical model of orientational alignment and, thus, it is a model-free approach. This approach intrinsically is not a physical model. It is a method of measurement of an orientation distribution function by means of EPR spectroscopy.

5. The approaches OD and OP seem to be rather close at a first sight. Both approaches comprise the expansion in a series of spherical Wigner D-matrix elements. Indeed, Eq. (3) is reduced to Eq. (1) in the case of slight orientation alignment, when $\exp(-U(\Omega)/k_bT_0) = 1 - U(\Omega)/k_bT_0$. On the other hand, these formulas demonstrate different behavior in the case of well-ordered media. Let the orientation distribution function be defined by Eq. (4) with coefficients c_{20} and c_{22}. The expansion of this function in the series (Eq. (1)) gives an infinite number of non-zero coefficients (order parameters). The examples of such expansion are presented in Table 1.

And *vice versa*, the orientation distribution function, specified by Eqs. (1) and (2), generates infinite number of coefficients c_{jm} for adequate description (Table 1, column 4)). Important difference of these two situations is the convergence of the sequences to the distribution functions. The slower convergence of OP expansion (Eqs. (3) and (4)) relative to OD approach (Eqs. (1) and (2)) is illustrated in Fig. 2. The functions, presented in Fig. 2, correspond to columns 2 and 4 in the Table 1 (column a and b in Fig. 2, respectively). It is seen, that the expansion of rank 6 is sufficient, when the OD approach is used. In the case of OP expansion of rank 6 is insufficient for correct description of orientation distribution (Fig. 2, column b).

Table 1
Representation of orientation distribution function defined by Eqs. (3) and (4) in the set of order parameters (columns 2 and 3) and representation of orientation distribution function defined by Eqs. (1) and (2) in the set of coefficients c_{jm} (column 4).

j,m	A^j_m for ODF specified by Eqs. (3) and (4), $c_{20} = 3.0$, $c_{22} = 3.0$	A^j_m for ODF specified by Eqs. (3) and (4), $c_{20} = -1$, $c_{22} = -1$	c_{jm} for ODF specified by Eqs. (1) and (2), $A^2_0 = -0.2, A - 2^2 = -0.2$
2.0	0.336	−0.205	−0.333
2.2	0.193	−0.229	−0.498
4.0	0.117	0.0398	−0.100
4.2	0.0922	0.0400	−0.241
4.4	0.0692	0.0465	−0.0825
6.0	0.0400	−0.00629	−0.0476
6.2	0.0359	−0.00624	−0.163
6.4	0.0283	−0.00623	−0.0461
6.6	0.0241	−0.00729	−0.0216

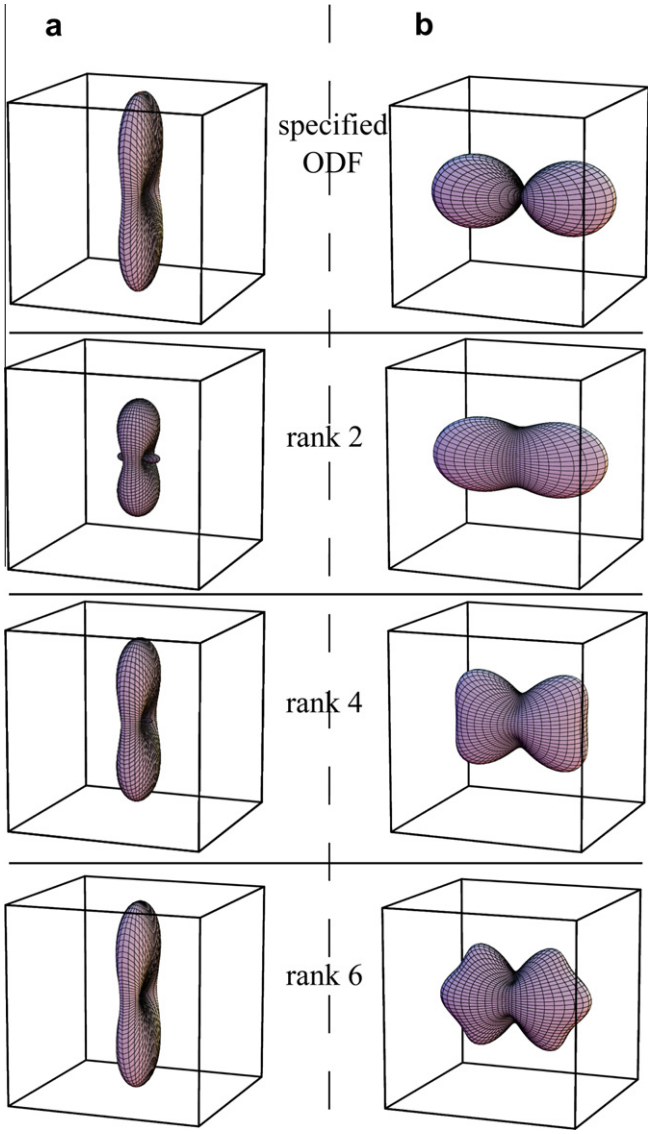

Fig. 2. The convergence of expansions Eqs. (1) and (2) and Eqs. (3) and (4) to the specified ODFs, (a) the approximations of ODF, specified by Eqs. (3) and (4) $c_{20} = 3.0$, $c_{22} = 3.0$, using expansion Eqs. (1) and (2); (b) the approximations of ODF, specified by Eqs. (1) and (2) $A_0^2 = -0.2, A_2^2 = -0.2$, using expansion Eqs. (3) and (4).

Origin of this difference is the following. The Eqs. (1) and (2) are the sequences of orthogonal functions. It is well known, that sequence of orthogonal functions converges uniformly and it is the best approximation (gives the least mean-squares deviations) in comparison with other sequences with the same rank (see, for example, [27]). The orientation distribution functions (Eqs. (1) and (2)) are normalized, if the first coefficient is equal to unity $\langle D_{00}^{0*} \rangle = a_{00} = 1$. All coefficients of the expansion are independent. On the other hand, the orientation distribution function (Eq. (3)) can be represented as follows:

$$In[\rho(\beta,\gamma)] = \sum_{j,m} c_{jm} D_{0m}^{j}(\beta,\gamma) - In\left[\int_{\Omega} d\Omega \exp\left[\sum_{j,m} c_{jm} D_{0m}^{j}(\beta,\gamma)\right]\right] \quad (11)$$

One can see that the Eq. (11), substantially is the expansion of logarithmic function. This function has a singularity in zero point. When the well-oriented molecular ensembles are considered, the angular distribution contains angular ranges with almost zero probability density of the molecular orientation. As a result large number of expansion terms is necessary to describe the orientation distribution functions.

One more drawback of OP approach is seen in expression Eq. (11) as the last summand. It is normalization coefficient that depends on all expansion coefficients and, consequently, makes each expansion coefficient dependent on every other one. This feature can be exemplified by the following situation. Let two order parameters A_0^2, A_2^2 be known from experimental measurements or molecular dynamics calculations and let the parameters be determined with ±5% tolerance: $A_0^2 = 0.337 \pm 0.017, A_2^2 = 0.194 \pm 0.0097$. The problem of determination of c_{20}, c_{22} values using the known values of order parameters is considered in [23]. This problem implies numerical solving of two nonlinear equations. The field of c_{20}, c_{22} values, compatible with given values of order parameters, is shown in Fig. 3.

One can see that simultaneous determination of two related parameters c_{20}, c_{22} leads to large uncertainty of results. This uncertainty can be reduced, if the experimental results (for example, shape of EPR spectra) contain information about additional order parameters. On the other hand, the value of any additional order parameter possibly will be inconsistent with the range of c_{20}, c_{22}, determined by values of two order parameters, that already have been used. It means that three or more nonlinear equations in two variables can be an inconsistent system. Adequate determination of c_{20}, c_{22} values seems to be possible only when the orientation distribution is really defined by potential with simple harmonic shape. Presumably, the uncertainty of determination of greater number of related values c_{jm} is even bigger than for c_{20}, c_{22}.

6. Higher order parameters ($A_2^2, A_0^4, A_2^4, A_4^4$ and others) are measured at present time (see, for example, [28]) to reveal fine details of orientation distribution function and to verify theoretical models. EPR technique is potentially applicable for these measurements. However, the OP approach cannot give independent values of the higher order parameters, since two determined values c_{20}, c_{22} define the whole set of order parameters.

7. The apparent advantage of the OP approach is the positivity of the orientation distribution function, which is ensured by the Boltzmann equilibrium. This model can provide values of the order parameters within physically meaningful ranges only. Indeed, the physical model must give reasonable values. On the other hand this advantage turns into drawback when the method of measurement is considered. Measurements must give meaningless results when incorrect conditions are used. The direct expansion of orientation distribution function (OD approach) is really a model-free method

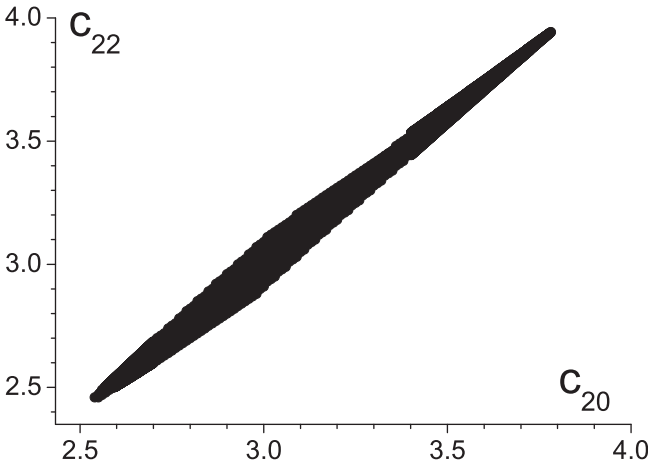

Fig. 3. The field of parameters c_{20}, c_{22} of orientation distribution function (Eqs. (3) and (4)) produced by the order parameters $A_0^2 = 0.337 \pm 0.017, A_2^2 = 0.194 \pm 00097$.

of determination of orientation distribution function from experimental EPR spectra. This procedure must give the meaningless results when erroneous spectra are treated, or mistaken magnetic parameters are used, or orientational relaxation in the course of spectra recording takes place, etc. Meaningless value is an indication of incorrect experimental conditions that is ordinary in case of other techniques of measurements. We believe that physical models of molecular orientation should be applied after the unbiased determination of orientational characteristics. Only in this case the applied models can be confirmed or disproved.

The problem of the model-free determination of orientational distribution, of course, is more complicated than the determination of parameters of a known model. The troubles concerning false local minima, including the minima with the meaningless parameters and negative distribution function, are more serious. The examples of overcoming of these troubles will be presented below.

3. Numerical consideration. Experimental examples

Let us consider the examples of application of the OD and OP approaches.

3.1. Example 1

Spin probe *R*1, shown in Fig. 4, was dissolved in liquid crystal 4′-pentyl-4-cyanobiphenyl (5CB). This probe can be used in *trans*- and *cis*-forms of the azobenzene moiety. To prepare aligned samples stretched porous polyethylene film was used. Elongated pores of this material induce the uniaxial orientation of liquid crystal embedded in it [29,30]. More experimental details are available in the Section 4.

EPR spectra, recorded at 77 and 295 K for different angles between direction of magnetic field of the spectrometer and the anisotropy axis of the sample, are shown in the Figs. 5 and 6 respectively.

Details of spectra simulation procedure are given below in the Section 4. The discrepancies between the best fit spectra and the experimental ones are given in Table 2. The ranks (column 1, Table 2) correspond to different truncation of the series (Eq. (1)) used in the fitting procedure.

Results of the fitting of the 77 K spectra using OD approach with rank 2 and 4 are illustrated in Fig. 7. One spectrum of the angular dependence is shown. One can see that the results of fittings with expansion rank 2 and 4 are very close visually. The use of the rank 4 leads to slight improvements in the lineshape and position of the outermost spectrum components (marked by arrows). However, as far as the 10–12 spectra, recorded at different angles, are simulated jointly these small improvements are accumulated and result in noticeable decrease of total discrepancy (see Table 2). Thus, we

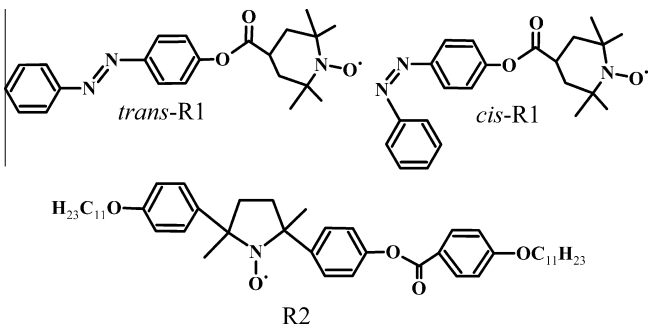

Fig. 4. Molecular structure of the spin probes used.

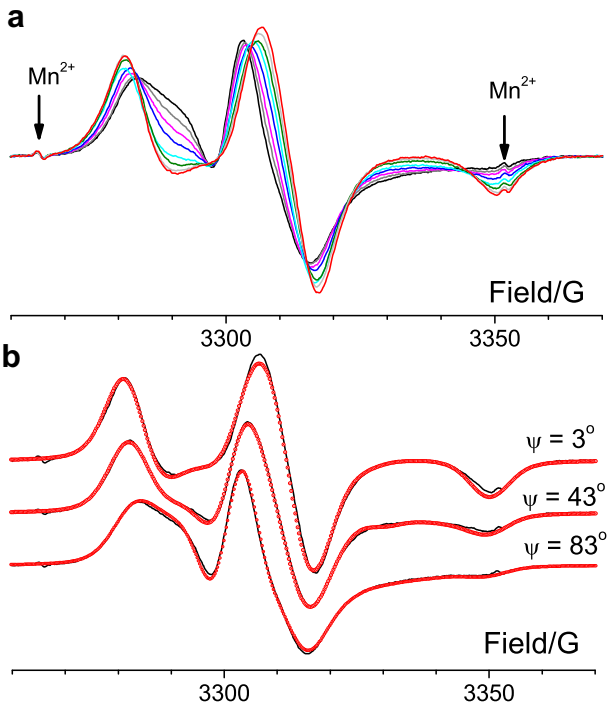

Fig. 5. (a) Experimental *X*-band (9.3 GHz) EPR spectraof probe *R*1 in 5CB embedded in porous polyethylene film for different angles between the film axis and magnetic field of spectrometer, 77 K; (b) examples of simulation, lines – experiment, dots – the best fitting within OD approach.

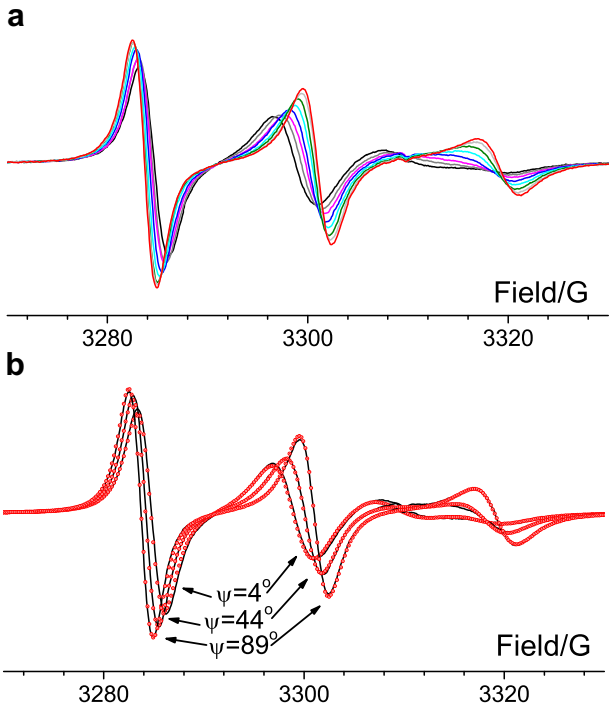

Fig. 6. (a) Experimental *X*-band (9.3 GHz) EPR spectra of probe *R*1 in 5CB embedded in porous polyethylene film for different angles between the film axis and magnetic field of spectrometer, 295 K; (b) examples of simulation, lines – experiment, dots – the best fitting within OP approach.

conclude, that value of discrepancy is a sensitive and reliable characteristic of validity of parameters, varied in the course of fitting. It is clear, that improvement of fitting should be considered

Table 2
Discrepancies between the experimental spectra and best fits.

Rank	Spectra at 77 K (Fig. 5a) fitted using OD approach	Spectra at 295 K (Fig. 6a) fitted using OP approach
2	1.78×10^{-9}	4.94×10^{-8}
4	1.29×10^{-9}	4.61×10^{-8}
6	1.26×10^{-9}	[a]
Error level	1.9×10^{-11}	1.8×10^{-9}

[a] The software of the OP approach does not permit expansion rank more than 4.

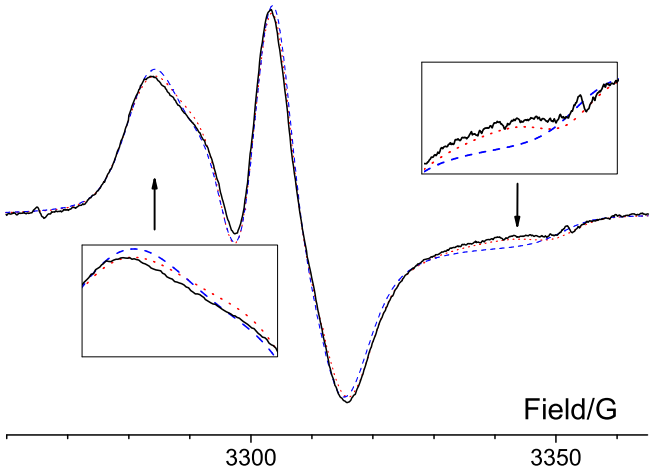

Fig. 7. One experimental spectrum from the set of spectra shown in Fig. 5a (solid line) and spectra calculated in the course of joint fitting of whole set with use of expansion ranks 2 (dashed line) and 4 (dotted line) within OD approach.

as meaningful, when decrease of discrepancy is more than the level of errors. In general there are more than one source of experimental errors related to recording of EPR spectra: noise of spectrometer, nonlinear baseline, errors of angle setting for aligned samples, etc. Commonly only noise level of spectrometer is estimated in experiments and used in analysis of EPR spectra. This value is obtained from the variance of a linear fit to the two baseline segments at either end of the spectrum [6]. Such values for our experiments are presented in Table 2 (last row) as an error level. The comparison of discrepancy diminishing with level of errors can be considered as a criterion of parameter validity. The Table 2 (column 2) shows, that the expansion rank 4 is required for description of 77 K spectra using Eqs. (1) and (2). It is seen as well, that addition of expansion member of rank 6 results in less significant improvement of fitting, and possibly should be considered as redundant.

The spectra in the Fig. 5a and Fig. 7 were simulated in simplifying assumption of uniaxial symmetry of molecular orientation frame (MOF). In accordance with Eq. (10) the essential parameters in this case are A_0^2, A_0^4, φ and θ, where $\Omega_{gF\to 9} \equiv (\phi, \theta, 0)$. In the course of simulation the values of a_{20}, a_{40}, φ, θ were varied. Order parameters A_0^2, A_0^4 were calculated using Eq. (2a). The spectra in the Fig. 6 were simulated using the OP distribution with the variation of the following parameters:

(i) coefficients of orienting potential c_{20} and c_{22};
(ii) angles φ and θ, that define the rotation and orientation molecular frame (MOF coincides with RF within the OP model, $(\phi, \theta, 0) \equiv \Omega_{gF\to MOF} \equiv \Omega_{gF\to RF}$);
(iii) coefficients of rotational diffusion $Rx = Ry$, Rz (uniaxial approximation).

The results are presented in the Table 3 and Fig. 8.

The data, presented in Table 3, and the functions, shown in Fig. 8, demonstrate the qualitative agreement between the data, obtained within the OD and OP approaches. However, there are following differences:

(i) The tilt angles θ, presented in Table 3 for these two functions, are somewhat different: 86.8° and 106.4°. According to the OD approach the angles θ and φ reflect position of the principal orientational axis of the probe in the frame gF. According to OP approach these angles reflect direction of the axis of fastest rotation in the frame gF. In the case under consideration principal orientational axis and principal rotation axis are close and approximately coincide with the long molecular axis (Fig. 4) that approximately lies along NO bond (X axis of g-tensor).
(ii) The function in the Fig. 8a is symmetrical in regard to its own axis (has uniaxial symmetry), whereas the function in the Fig. 8b is slightly flattened. This feature is described by nonzero value of c_{22} coefficient. Nonzero value of c_{22} is ordinarily interpreted as biaxiality of the medium. But in the case under consideration it means only, that the real orientation frame (MOF) in the considered probe is tilted relative to the rotation frame, taken in OP model (see the topic 3 above). Nonzero c_{22} coefficient arises in accordance with the Eq. (10), although this distortion is small in this case.
(iii) The values of order parameters (Table 3, last row), obtained using OD and OP approaches, are considerably different.

In general, the characteristics of the ODF, obtained using OD and OP approaches, are similar in spite of different temperatures. It

Table 3
The ODF parameters, obtained by simulation of EPR spectra of the probe *R*1 in *trans*-form presented in the Fig. 6a and b.

ODF parameters at 77 K (spectra in Fig. 6a) fitted using OD approach[a]	ODF parameters at 295 K (spectra in Fig. 6b) fitted using OP approach[a]
$a_{20} = 1.88 \pm 0.02$	$c_{20} = 1.239 \pm 0.007$
$a_{40} = 0.53 \pm 0.03$	$c_{22} = -0.080 \pm 0.002$
	$Rx = Ry = (1.22 \pm 0.02) \times 10^7$;
	$Rz = (6.47 \pm 0.07) \times 10^8$
$\varphi = 11.9° \pm 0.7°$	$\varphi = 10.2° \pm 0.3°$
$\theta = 86.8° \pm 2.2°$	$\theta = 106.4° \pm 0.2°$
$A_0^2 = 0.376$	$A_0^2 = 0.275$; $A_2^2 = -0.010$;
$A_0^4 = 0.059$	$A_0^4 = 0.050$; $A_2^4 = -0.0029$;
	$A_0^6 = 0.0065$

[a] The square roots for diagonal elements of covariance matrix in the final point of minimization are presented here and below as errors. For more details see Section 4.

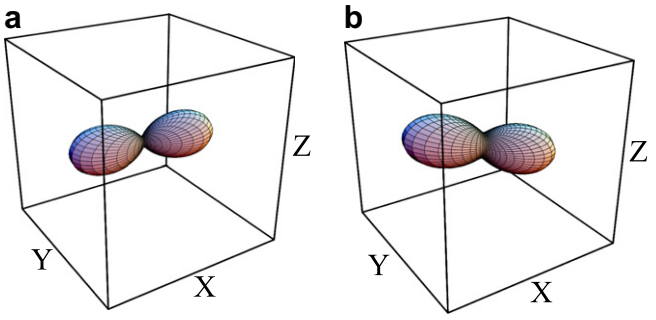

Fig. 8. The orientation distribution functions determined in the course of simulation of: (a) EPR spectra, shown in Fig. 5a and (b) EPR spectra, shown in Fig. 6a.

Table 4
ODF parameters obtained by simulation of EPR spectra of the probe *R*1 in *cis*-form.

ODF parameters at 77 K obtained using OD approach	ODF parameters at 295 K obtained using OP approach, rank 2[a]	ODF parameters at 295 K obtained using OP approach, rank 4[a]
Discrepancy 5.62×10^{-9}	Discrepancy 5.25×10^{-8}	Discrepancy 4.74×10^{-8}
Error level 3.0×10^{-11}	Error level 1.3×10^{-9}	Error level 1.3×10^{-9}
$a_{20} = 1.03 \pm 0.02$	$c_{20} = 0.23 \pm 0.002$; $c_{22} = -0.14 \pm 0.001$	$c_{20} = 0.231 \pm 0.002$; $c_{22} = -0.121 \pm 0.001$
$a_{40} = 0.17 \pm 0.02$		$c_{40} = 0.22 \pm 0.01$; $c_{42} = 0.17 \pm 0.01$;
		$c_{44} = 0.26 \pm 0.01$
	$Rx = Ry = (3.93 \pm 0.03) \times 10^7$;	$Rx = Ry = (3.95 \pm 0.02) \times 10^7$;
	$Rz = (5.37 \pm 0.08) \times 10^8$	$Rz = (5.50 \pm 0.1) \times 10^8$
$\varphi = -42.4° \pm 0.3°$	$\varphi = 6.3° \pm 0.9°$	$\varphi = 5.4° \pm 0.08°$
$\theta = 86.1° \pm 2.8°$	$\theta = 91.7° \pm 1.1°$	$\theta = 90.0° \pm 1.2°$
$A_0^2 = 0.206$	$A_0^2 = 0.046$	$A_0^2 = 0.046$

[a] Error values obtained in the course of these calculations seem to be incredibly small.

means that as a result of the fast cooling the liquid crystal 5CB passes into supercooled state that mainly retains the molecular order of liquid crystalline state. When cooling of a sample is not fast enough, intermediate cases of partial orientational relaxation can be observed [19]. These results illustrate the topic 1, discussed above.

3.2. Example 2

Similar experiments were carried out for *cis*-isomer of the probe *R*1. For that purpose the sample was irradiated by light to stimulate the *trans-cis* isomerization of the probe molecules. The EPR spectra, obtained in such experiments, are very similar to the spectra, presented in example 1, but demonstrate some weaker angular dependence. The results of ODF determination are presented in Table 4 and Fig. 9.

It is seen, that obtained orientation distribution functions are quite different. The direction of symmetry axis of ODF, obtained using OD approach (Fig. 9a), is in accordance with bent shape of the probe molecule in *cis*-form (Fig. 4). The value of order parameter $A_0^2 = 0.206$ is in accordance with the optical linear dichroism of the sample studied.[1]

The functions, determined using OP approach for 2nd and 4th rank of the expansion, are presented in Fig. 9b and c, correspondingly. The direction of long axis of the ODF takes the orientation parallel to *X* axis of gF. However, the shape of the function has no clear physical interpretation. Very small value of order parameter is in contradiction with the liquid crystalline nature of the medium. The addition of the 4th rank of the expansion does not improve the results. Origin of this failure is the considerable deviation of the molecular orientation frame (MOF) from the rotation frame (RF). The OP method actually visualizes the orientation degree of RF axis. When this axis lies near the orientational axis, the results are close to model-free determination of ODF, as it is shown above for the probe in *trans*-form. Thus, it is not surprising, that value of order parameter, obtained within the OP approach, does not describe the real molecular alignment (Table 4, last row).

These results exemplify the topic 3 presented above.

3.3. Example 3

In the examples, presented above, there was no problem of meaningless negative part of orientation distribution function that was discussed in the topic 7 . The simulations of the experimental EPR spectra led to the functions, which were positive at every point

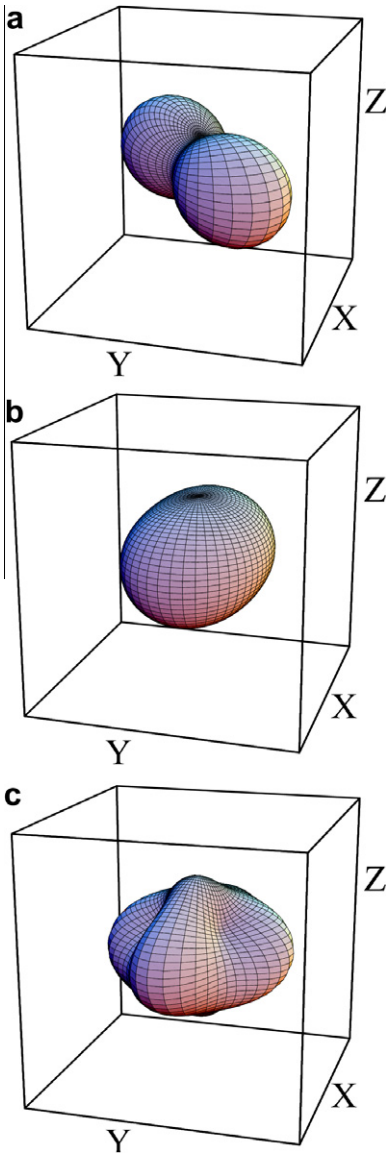

Fig. 9. Orientation distribution functions for probe *R*1 in *cis*-form: (a) at 77 K, determined within OD approach; (b) at 295 K, determined within OP approach with expansion rank 2; (c) at 295 K, determined within OP approach with expansion rank 4.

[1] The values of linear dichroism *d* measured by means of recording of UV-vis spectra in polarized light in the range of $n\pi^*$ and $n\pi^*$ absorption bands (350–450 nm) were found to be in the ranges 0.30 ÷ 0.39 and 0.19 ÷ 0.26 for *trans*- and *cis*-form of probe, respectively.

of angular space independently on initial values of ODF parameters. Here we present the example, in which determination of completely positive orientation distribution function requires special efforts. This example was obtained using the probe *R*2, shown in the Fig. 4. The probe was dissolved in liquid crystal 5CB, which was aligned in pores of porous polyethylene as described in Section 4.

Angular dependences of EPR spectrum were recorded at 77 K and at 293 K. Several experimental spectra, as well as the results of their simulation, are presented in the Fig. 10. Simulation of the spectra, recorded at 77 K using OD approach, has led to distribution function, having a small negative part. The absolute value of this function is shown in the Fig. 11a. The negative part of the function forms a "skirt" in the area, where probability density of particles is near zero.

To obtain a completely positive orientation distribution, penalty function was used in the course of spectra simulation. The penalty value was calculated by the following expression:

$$F = K \cdot Neg = K \cdot \frac{\int_\Omega |\rho(\beta,\gamma)| d\Omega - \int_\Omega \rho(\beta,\gamma) d\Omega}{2 \int_\Omega |\rho(\beta,\gamma)| d\Omega} \quad (12)$$

where *Neg* is negative fraction of distribution function.

Function *F* is similar to quadratic penalty function, proposed in [31] as a penalty function for "external point" method. Such functions are applied to achieve optimal solution in the case, when the iteration movement occurs through the forbidden area of varied parameters. The value of *F* increases with negative part of ODF, hence introduction of this function to the minimization function guides the iteration procedure aside from unwanted area of parameters. Variation of coefficient *K* allows one to minimize the negative fraction of distribution function, but not to distort the distribution shape.

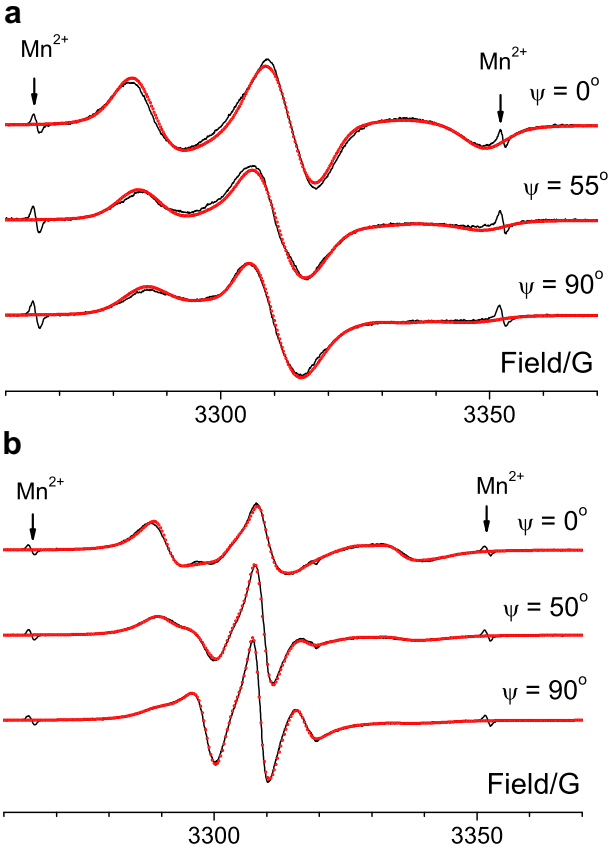

Fig. 10. Experimental *X*-band (9.3 GHz) EPR spectra of probe *R*2 in 5CB embedded in porous polyethylene film for different angles between the film axis and magnetic field of spectrometer (lines) and the best fitting (points): (a) within OD approach, 77 K; (b) within OP approach, 293 K.

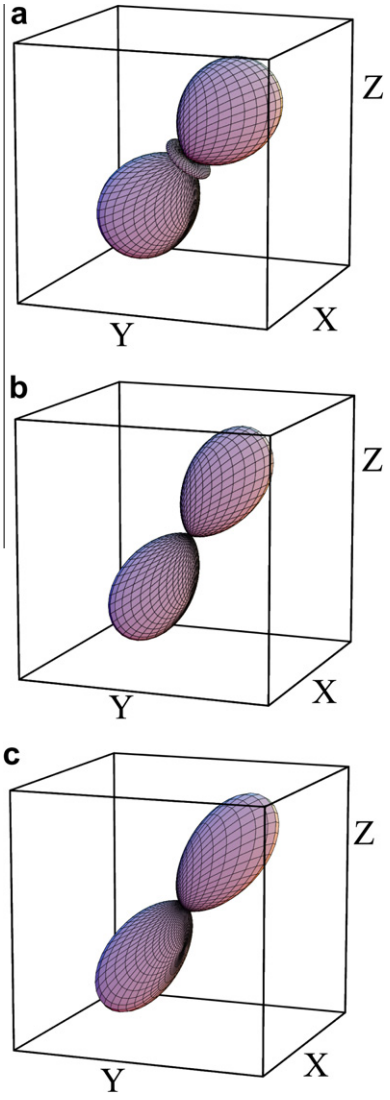

Fig. 11. Orientation distribution functions of *R*2 probe in liquid crystal 5CB; (a) 77 K, ODF has negative part, (b) 77 K, ODF is positive in all angular space, (c) 293 K, ODF determined using OP approach.

The results of minimization procedure with use of different penalty values are presented in Table 5. One can see that use of penalty function really leads to reduction of the negative part of distribution function to the level, caused by experimental errors. It is seen as well that optimal values of parameters $(a_{20}, a_{40}, \theta, \varphi)$ converge to certain values, that do not depend on *K* value within experimental errors. The resulted distribution function is shown in Fig. 11b. One can see from Table 5 that the penalty causes some increase of discrepancy between experimental and calculated EPR spectra. However, the spectra, calculated with and without penalty function, almost coincide visually.

Use of the OP approach for simulation of spectra, recorded at 293 K, led to the following optimal parameters: $c_{20} = 2.22 \pm 0.15$, $c_{22} = 0.32 \pm 0.05$, $Rx = Ry < 1 \times 10^6$, $Rz = (2.12 \pm 0.05) \times 10^8$, $\theta = 40.7° \pm 0.4°$, $\varphi = 109.3° \pm 1.0°$. The distribution, corresponding to these parameters, is shown in Fig. 11c. It is seen, that in this case the functions, obtained within OD and OP approaches, are visually almost the same. Values of order parameters A_2^0 and A_4^0 are similar

Table 5
The ODF parameters, obtained by simulation of EPR spectra of probe *R*2 at various magnitudes of the penalty function.

K	0	1	2	5	15	150
Neg	0.157	2.4×10^{-4}	2.5×10^{-5}	1.0×10^{-6}	6×10^{-8}	0.0
a_{20}	3.62 ± 0.08	2.611 ± 0.016	2.608	2.608	2.608	2.608
a_{40}	−0.27 ± 0.05	0.801 ± 0.079	0.808	0.810	0.810	0.810
θ	40.49 ± 0.34	33.58 ± 0.16	33.54	33.53	33.53	33.53
φ	96.6 ± 3.8	90.29 ± 1.35	90.29	90.29	90.30	90.29
Discrepancy	1.114×10^{-8}	1.256×10^{-8}	1.256×10^{-8}	1.257×10^{-8}	1.257×10^{-8}	1.257×10^{-8}

Table 6
Dependence of negative part of orientation distribution from deviations of *g*-values and Az value.

Shift of g-value δ	Negative portion of distribution	Shift of Az value, *G*	Negative portion of distribution
+0.0002	0.0	−1.0	0.0
+0.0005	0.0	−2.0	0.0
+0.001	0.113	−4.0	0.354
+0.002	0.342	−8.0	0.299
−0.0002	0.0	+1.0	0.0
−0.0004	0.058	+2.0	0.059
−0.001	0.304	+4.0	0.197
−0.002	0.468	+8.0	0.340

as well. This accordance is a result of vicinity of directions of principal orientation axis and fastest rotation axis of the probe molecule.

The system, described in this example, is more aligned then the systems, presented above in examples 1 and 2. Indeed, the order parameter A_2^0 in the example 3 is equal to 0.52, that is essentially more than the values 0.376 and 0.206 for *R*1 in *trans*- and *cis*- forms (examples 1 and 2). As a result of stronger alignment the orientational distribution has angular ranges with very low probability density of particle orientations. Small experimental errors can lead to the negative probability density in these angular ranges, that means the appearance of negative fraction of orientation distribution. We suppose, that negative parts of distribution would be obtained more often when strongly aligned systems are considered. This trouble can be easily overcome by use of the penalty function. On the other hand the large negative fraction, retained in the presence of penalty, means that experimental spectra or Hamiltonian parameters used are essentially erroneous. The illustration of this statement is presented in the Table 6. Determinations of orientation distribution were carried out for EPR spectra from example 1 (Fig. 5) with deviated *g*-values and Az value. The g_x and g_z values were simultaneously shifted to $g_x + \delta$ and $g_z - \delta$, respectively. One can see from Table 6 the appearance of negative parts of orientation function with deviation of magnetic parameters from correct values.

3.4. Example 4

The instructive examples of using OP and OD approaches can be obtained by treatment of the experimental data, described in [22]. The far-infrared EPR spectra (250 GHz) of nitroxide-labeled cholesterol (CSL) in macroscopically aligned dimyristoylphosphatidylcholine/dimyristoylphosphatidylserine mixture bilayer membrane (DMPC/DMPS 80:20), presented in [22], are shown in Fig. 12.

The authors of [22] have successfully simulated the experimental spectra using parameters, given in the Table 7 (column 1). From analysis of the spectra the authors concluded, that rotational motions in this case are frozen out in the 250-GHz EPR time scale. The coincidence of g-tensor frame (gF), molecular orientation frame (MOF) and rotation frame (RF) was assumed in the course of the simulation.

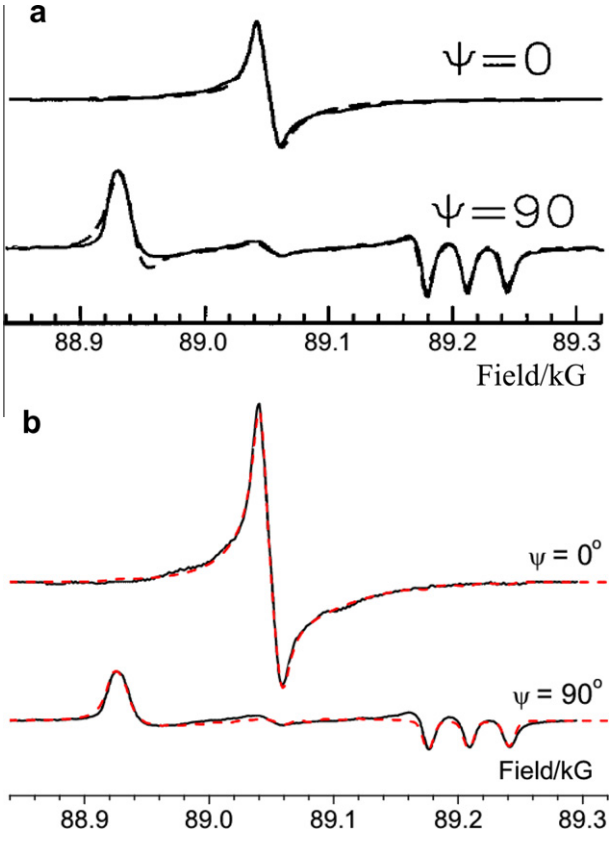

Fig. 12. (a) 250 GHz EPR spectra of CSL probe in DMPC/DMPS 80:20 bilayer (solid lines) and simulated spectra (dashed lines), taken from [21], (b) spectra simulated within OD approach.

There is an opinion, that motionless EPR spectra (rigid limit) can be simulated applying SLE in the limit of very low diffusion rates. Quantitative calculations, however, do not confirm this statement. EPR spectra, calculated for different rotational diffusion coefficients, are presented in the Fig. 13 in comparison with the rigid limit spectra. The parameters for these calculations are taken from [22] (Table 7, column 1). It is seen that positions and widths of spectral components approach the positions and widths of rigid limit spectra, but do not reach desirable limit. Further decrease of diffusion rates is really impossible, since the basis set, required for convergence of the ESR lineshapes, becomes impractically large. Values of $R < 10^5\ s^{-1}$ correspond to truncation numbers *L*max, *K*max, and *M*max $\geqslant$ 50 [5,22]. As far as we know, there are no examples of calculation with bigger truncation values in literature. Thus, application of SLE programs for simulation of rigid limit spectra is very time-consuming and does not give reliable quantitative results.

Please cite this article in press as: A.Kh. Vorobiev et al., Chem. Phys. (2012), http://dx.doi.org/10.1016/j.chemphys.2012.10.006

Table 7
Parameters obtained by simulation of spectra in Fig. 12.

Parameters of OP approach fitting of the spectra in Fig. 12a, data from [22]	Parameters of OP approach fitting of the same spectra with diffusion tilt, data from [22]	Parameters of OD approach fitting of the spectra in Fig. 12b, rank 6	Parameters of OD approach fitting of the same spectra with rank 8
–	–	Discrepancy 3.44×10^{-11}	Discrepancy 3.12×10^{-11}
–	Tilt RF relative gF $\beta_D = 13°$	Tilt MOF relative gF $\varphi = 101.9° \pm 0.2°$ $\theta = 111.1° \pm 0.6°$	Tilt MOF relative gF $\varphi = 99.8° \pm 0.2°$ $\theta = 110.7° \pm 1.0°$
Rotational diffusion: $Rx = 2 \times 10^5$; $Ry = 7 \times 10^6$; $Rz = 1 \times 10^7$; $c_{20} = -0.81$ $c_{22} = -1.47$	Rotational diffusion: $Rx = 2 \times 10^5$; $Ry = 1 \times 10^6$; $Rz = 2 \times 10^7$; $c_{20} = -0.36$ $c_{22} = -2.00$	Libration angles: $L_x = 0.1°$ $L_y = 13.3°$ $L_z = 12.7°$ $a_{20} = 3.33 \pm 0.07$ $a_{40} = 3.03 \pm 0.20$ $a_{60} = 1.56 \pm 0.13$	Libration angles: the same $a_{20} = 3.17 \pm 0.06$ $a_{40} = 2.51 \pm 0.16$ $a_{60} = 1.38 \pm 0.16$ $a_{80} = 0.64 \pm 0.06$
$g_{xx} = 2.00871$ $g_{yy} = 2.00573$ $g_{zz} = 2.00210$ $A_{xx} = 4.9$ $A_{yy} = 5.5$ $A_{zz} = 33.1$	The same	$g_{xx}^{av} = 2.008547$ $g_{yy}^{av} = 2.005777$ $g_{zz}^{av} = 2.002217$ $A_{xx}^{av} = 5.399$ $A_{yy}^{av} = 5.498$ $A_{zz}^{av} = 32.60$	The same

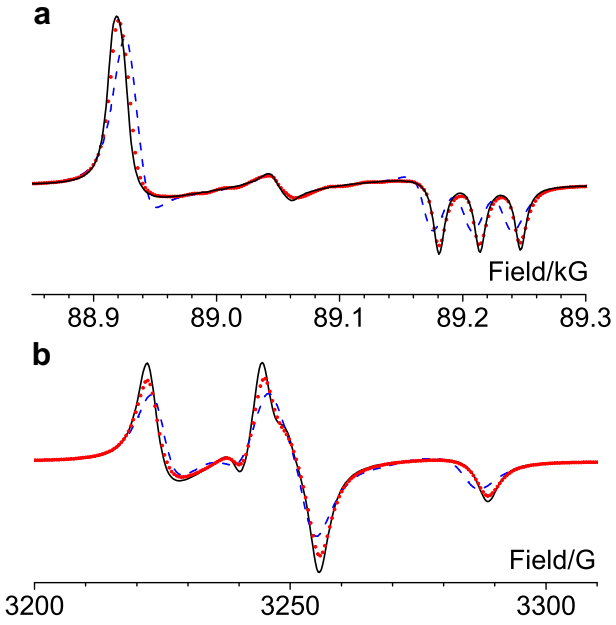

Fig. 13. (a) EPR spectra at 250 GHz, calculated in rigid limit (solid line) and spectra calculated using SLE program for isotropic diffusion coefficients $5 * 10^5$ s^{-1} (dotted line), $5 * 10^6$ s^{-1}(dashed line); (b) EPR spectra at 9.1 GHz calculated in rigid limit (solid line) and spectra calculated using SLE program for isotropic diffusion coefficients $1 * 10^5$ s^{-1} (dotted line), $5 * 10^6$ s^{-1}(dashed line); truncation values are: *L*max = 46, *K*max = 44, and *M*max = 30.

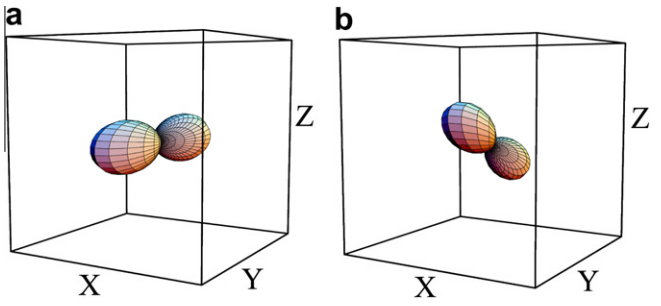

Fig. 14. Orientation distribution functions obtained by simulation of spectra in Fig. 10: (a) using OP approach (parameters in column 1 of Table 6); (b) using OD approach (parameters in column 3 of Table 6). The functions are presented in g-tensor frame (gF).

The presented results demonstrate, that the experimental as well as simulated spectra in Fig. 12a are not strictly rigid limit spectra. They are slightly changed by slow rotation. It is an obstacle for using OD approach, because the methods utilizing Eqs. (1) and (2) for rotating molecules are not developed at present time. Fortunately, in the case considered, the rotation influence is rather small and mainly consists in some shift of the spectral components. The shift can be approximately described in the framework of libration model. The librations around axes of g-tensor frame (gF), that average partially magnetic parameters, were used for description of spectra in the present work. It was found, that small amplitudes of librations $L_x = 0.1°$, $L_y = 13.3°$ and $L_z = 12.7°$ are sufficient to describe the spectra quantitatively. The values of magnetic parameters, partially averaged by these librations, are presented in Table 7 (columns 3).

Results of the spectra simulations using the approaches OP and OD are quite similar (Fig 12a and b). The orientation distribution functions, determined by means of the simulation, are shown in Fig 14, and optimal values of parameters are collected in Table 7.

The optimal parameters demonstrate the following advantages and the weaknesses of both approaches:

(i) The orientation distribution function, obtained using OP approach, is positive in each point. The optimal function, obtained using OD is positive as well. However, depending on the initial point of minimization, the fitting procedure in the case of OD approach can pass or not pass through parameters ranges with negative distribution function. Thus, use of penalty function is not necessary, but is desirable.

(ii) Authors of [22] expected from the analysis of geometry of the probe molecule, that the orientational direction of the probe is tilted by 13° in respect to g_y axis. The OP model, applied in [22], was unable to determine this tilt since very similar spectra are produced with different sets of parameters (columns 1 and 2 in Table 7). On the other hand one can see from the Table 7, that the tilt of the rotational diffusion frame very noticeably influences parameters of orientation distribution function. Indeed, optimal values of c_{20} and

Table 8
Values of order parameters, calculated using the parameters from Table 7.

Eqs. (3) and (4), c_{20} = 2.205 c_{22} = 0.239, correspond to col. 1 in Table 7[a]	Eqs. (3) and (4), c_{20} = 2.629 c_{22} = 0.78, correspond to col. 2 in Table 7[a]	Eqs. (1) and (2), correspond to col. 3 in Table 7	Eqs. (1) and (2), correspond to col. 4 in Table 7
A_0^2 = 0.476;	A_0^2 = 0.530;	A_0^2 = 0.67 ± 0.014	A_0^2 = 0.64 ± 0.012
A_{02}^2 = 0.018;	A_2^2 = 0.048;	A_0^4 = 0.337 ± 0.020	A_0^4 = 0.279 ± 0.018
A_0^4 = 0.149;	A_0^4 = 0.191;	A_0^6 = 0.120 ± 0.010	A_0^6 = 0.106 ± 0.012
A_2^4 = 0.011;	A_2^4 = 0.036;		A_0^8 = 0.038 ± 0.0004
A_0^6 = 0.034;	A_0^6 = 0.052;		
A_2^6 = 0.004;	A_2^6 = 0.015;		
A_0^8 = 0.006;	A_0^8 = 0.011;		
A_2^8 = 0.0009;	A_2^8 = 0.0045;		

[a] The other values of A_m^l were less than 10^{-3} and are not shown

c_{22} with and without the tilt demonstrate large difference. This difference first of all is the result of change of MOF on tilting of RF as RF ≡ MOF in OP approach. Secondly, the difference indicates the instability of the results, discussed above (topic 6).

(iii) Order parameters, that have been calculated using the values from Table 7, are presented in Table 8. The order parameters, obtained using OP and OD approaches, can be compared only if the values are given in the same coordinate frame. Therefore, the values c_{20} and c_{22} were converted using y-ordering (i.e., permuting magnetic axes $y \to z'$, $z \to x'$, and $x \to y'$ [22]) before the calculation of order parameters.

Table 8 demonstrates, that two parameters (c_{20} and c_{22}) produce the infinite number of order parameters, but values of these order parameters cannot be considered as reliable or experimentally determined. One can see the biaxiality (nonzero A_m^l with $m \neq 0$ in columns 1, 2), that is the result of the incorrect choice of molecular orientation frame.

(iv) The model-free OD approach provides the values of higher rank order parameters, which presently cannot be determined by other experimental methods. This technique seems to be enough stable towards change of simulation procedure (compare column 3 and 4 in Tables 7 and 8).

This result is the illustration of topic 6, discussed above.

4. Experimental and computational details

4.1. Materials

Spin probe *R*1 (Fig. 3) was synthesized as described elsewhere [32,33], and was kindly granted by Prof. S. Nakatsuji (University of Hyogo). Spin probe *R*2 (Fig. 3) was synthesized as described in [34] and kindly granted by Prof. R. Tamura (Kyoto University).

Liquid crystal 4-n-pentyl-4′-cyanobiphenyl (5CB) from *Merck* was used without further purification. It forms nematic mesophase in temperature range 295–308 K [35].

Stretched porous polyethylene films with thickness of 0.05 mm were produced using the procedure, described in [36] and kindly granted by Prof. G.K. Elyashevitch (Institute of Macromolecular Compounds, Russian Academy of Sciences). Pores of this material with diameter ~200 nm are elongated mainly uniaxially. This porous polyethylene aligns liquid crystal, embedded into it, due to the orientational action of pores surface [29,30].

4.2. Sample preparation

Stretched porous polyethylene was used to induce alignment of liquid crystals. The direction of stretching is the direction of uniaxial alignment [30]. Spin probe was dissolved in liquid crystal 4′-pentyl-4-cyanobiphenyl to prepare the solution with concentration about 10^{-3} M. The solution was deposited on the film surface where it was readily soaked into the film due to the capillarity of pores. Excess of liquid crystal was thoroughly removed from the surface. Ten cuts of filled film were stacked and co-aligned to form sample with dimensions $\sim 1 * 4 * 15$ mm^3.

Trans-form of spin probe *R*1 was transformed to *cis*-form by irradiation of the sample with unpolarized light of high-pressure mercury lamp (λ = 365 nm).

4.3. EPR spectra recording

EPR spectra were recorded with *X*-band (9.3 GHz) EPR spectrometer Varian E3. Varian E-4557-9 temperature control unit (with accuracy of ±1 °C) was used to record the spectra at 295 K. For recording spectra at 77 K the sample was placed into Dewar vessel, filled with liquid nitrogen. EPR spectra were recorded at different angles between magnetic field vector and the sample anisotropy axis with 10° step. The sample was turned around the axis, perpendicular both to the magnetic field and to the sample anisotropy axis. Turn angles were set with accuracy ±0.5° using a goniometer. The set of spectra, obtained in the course of such procedure, is referred to as angular dependence.

All experimental spectra were plotted against magnetic field, measured in Gausses, and were corrected according to spectrometer base line. Each spectrum was normalized on the value of double integral. Experimental noise level was calculated as $\frac{1}{2}\sum\frac{I^2}{n}$, where n is number of points, I is the intensity of the spectrum, taken within the magnetic field ranges, where the signal of the spin probe was absent (at both end segments of the spectrum). These field ranges cover 10–15% of the spectral sweep width. The noise level was assumed to be constant for all the spectra of an experiment.

4.4. Linear dichroism measurement

Linear dichroism was calculated in accordance with the following expression:

$$d = (A_0^2)^{UV} = \frac{A_{||} - A_{\perp}}{A_{||} + 2A_{\perp}}$$

where $A_{||}$ and $A_{\perp}$ are absorbances at parallel and perpendicular polarization of light, relative to the sample director, respectively.

Absorbances at wavelengths 350 and 440 nm were measured using spectrophotometers SPECORD M40 with polarizing Glan prism. One layer of porous polyethylene film, filled with liquid

Table 9
Magnetic parameters of spin probes R_1[a] and R_2.

Spin probe	g_{xx}	g_{yy}	g_{zz}	A_{xx}	A_{yy}	A_{zz}
R_1	2.0092 ± 0.0002	2.0058 ± 0.0002	2.0019 ± 0.0002	6.9 ± 0.5	5.9 ± 0.6	33.8 ± 0.2
R_2	2.0090 ± 0.0002	2.0060 ± 0.0002	2.0020 ± 0.0002	4.0 ± 0.3	3.7 ± 0.3	32.1 ± 0.2

[a] parameters for R_1 in *trans*- and *cis*-configurations of the azobenzene moiety are the same.

crystal 5CB with dissolved spin probe *R*1 was used for the measurements.

Value of optical dichroism *d* is equal to order parameter of dipole transition moment direction of the photochromic molecule $(A_0^2)^{UV}$.

4.5. EPR spectra simulation

In the course of EPR spectra simulation the minimizing program NL2SOL [37] was used.

Errors of parameters determination were calculated on the basis of the covariance matrix and *t*-distribution statistics [38].

In the present work three kinds of simulation of EPR spectra were performed.

1. Simulation of EPR spectrum of the sample with stochastic orientation of paramagnetic molecules (disordered samples), recorded at 77 K, was carried out to determine magnetic parameters of spin probe in considered matrix. The calculation of ESR spectra was performed in rigid limit within the approximation of second order perturbation theory. The obtained magnetic parameters are presented in Table 9. In example 4 the literature values of magnetic parameters were used. The magnetic parameters, averaged by stochastic rotational oscillations of paramagnetic molecules (quasi-librations), were calculated using the expressions, presented in [39,40].
2. For analysis of angular dependence of EPR spectrum in rigid limit 9–12 EPR spectra, recorded at various orientations of the sample in magnetic field, were simulated jointly. Calculations were performed with assumption of axial symmetry of the probe orientation frame (MOF). ODF parameters and width of individual resonance line were varied in the course of simulation. All rigid limit simulations and determination of ODF were performed using home-made software, available at http://www.chem.msu.su/eng/lab/chemkin/ODF3/welcome.html. The program is described in detail in [3].
3. Analysis of EPR spectrum angular dependence at 295 K was performed using either the program [4], which was modified for joint simulation of series of EPR spectra, or the program NLSL (Version 1.5.1) [6]. The results of these simulations were identical.

5. Conclusions

The presented consideration and experimental examples demonstrate that the method of determination of orientation distribution function by analysis of EPR spectra, based on direct expansion of the function in a series of generalized spherical harmonics, is a model-free technique. It gives the unbiased characteristics of molecular distribution, including direction of orientational axis of probe molecule and high rank order parameters. Main drawback of the technique in present time is its inapplicability to the systems with high molecular mobility. *Vice versa*, in the commonly used method, based on the mean field potential and Boltzmann equilibrium, rotational molecular mobility is taken into account, but this method gives rather rough and unreliable characteristics of orientation distribution. Main weaknesses of this technique are the interdependence of determined parameters, assumption of identity of orientational and rotational molecular frames and coincidence of global and local orientational directors of the sample.

Acknowledgments

The authors acknowledge the financial support of Russian Foundation for Basic Research (Grant No. 12-03-31114). The authors thank Prof. S. Nakatsuji (University of Hyogo), Prof. R. Tamura (Kyoto University) for provision of paramagnetic probes and Prof. G.K. Elyashevitch for provision of stretched porous polyethylene films. This work was performed using 'Lomonosov' and 'Chebyshev' supercomputers of M.V. Lomonosov Moscow State University.

References

[1] C. Zannoni, Distribution function and order parameters, in: G.R. Luckhurst, G.W. Gray (Eds.), The Molecular Physics of Liquid Crystals, Academic Press, London, 1979, pp. 51–83.
[2] J. Michl, E.W. Thulstrup, Spectroscopy with Polarized Light: Solute Alignment by Photoselection, in Liquid Crystals, Polymers and Membranes, VCH Publishers, New York, 1986.
[3] A.Kh. Vorobiev, N.A. Chumakova, Simulation of rigid-limit and slow-motion EPR spectra for extraction of quantitative dynamic and orientational information, in: A.I. Kokorin, (Ed.), Nitroxides – Theory, Experiment and Applications, InTech, Rijeka, 2012, pp. 57–112. ISBN: 979-953-307-1090-0.
[4] J.H. Freed, Theory of slow tumbling ESR spectra for nitroxides, in: L.J. Berliner (Ed.), Spin Labeling: Theory and applications, Academic Press, New York, 1976, pp. 53–132.
[5] D.J. Schneider, J.H. Freed, Calculating slow-motional magnetic resonance spectra: a user's guide, in: L.J. Berliner, J. Reuben (Eds.), Biological Magnetic Resonance, vol. 8, Plenum, New York, 1989, pp. 1–76.
[6] D.E. Budil, S. Lee, S. Saxena, J.H. Freed, J. Magn. Reson. Series A 120 (1996) 155.
[7] G.R. Luckhurst, Mol. Cryst. Liquid Cryst. 21 (1973) 125.
[8] E. Meirovitch, D. Igner, E. Igner, G. Mora, J.H. Freed, J. Chem. Phys. 77 (1982) 3915.
[9] E. Meirovitch, J. Phys. Chem. 88 (1984) 2629.
[10] C.F. Polnaszek, J.H. Freed, J. Phys. Chem. 79 (1975) 2283.
[11] D. Xu, D.E. Budil, C.K. Ober, J.H. Freed, J. Phys. Chem. 100 (1996) 15867.
[12] R. Cassol, M.-T. Ge, A. Ferrarini, J.H. Freed, J. Phys. Chem. B 101 (1997) 8782.
[13] K. Khairy, D. Budil, P. Fajer, J. Magn. Reson. 183 (2006) 152.
[14] V. Barone, Phys. Chem. Chem. Phys. 8 (2006) 4609.
[15] M. Zerbetto, A. Polimeno, V. Barone, Comp. Phys. Commun. 180 (2009) 2680.
[16] K. Ajtai, A.R. French, Th.P. Burghardt, Biophys. J. 56 (1989) 535.
[17] Th.P. Burghardt, N.L. Thompson, Biophys. J. 48 (1985) 401.
[18] J. Caldeira, J.L. Figueirinhas, C. Santos, M.H. Godinho, J. Magn. Reson. 170 (2004) 213.
[19] A.Kh. Vorobiev, N.A. Chumakova, J. Magn. Reson. 175 (2005) 146.
[20] N.A. Chumakova, A.Kh. Vorobiev, Mendeleev Commun. 18 (2008) 21.
[21] N.A. Chumakova, D.A. Pomogailo, T.S. Yankova, A.Kh. Vorobiev, Mol. Cryst. Liquid Cryst. 540 (2011) 196–204.
[22] J.P. Barnes, J.H. Freed, Biophys. J. 75 (1998) 2532.
[23] M. Zerbetto, M. Buck, E. Meirovitch, A. Polimeno, J. Phys. Chem. B 115 (2011) 376.
[24] R.A. Marcus, N. Sutin, Biochim. Biophys. Acta 811 (1985) 265–322.
[25] A.I. Smirnov, Recent advances in ESR techniques and methods Employed in Nitroxide Experiments, in: G.I. Likhtenshtein, J. Yamauchi, Sh. Nakatsuji, A.I. Smirnov, R. Tamura (Eds.), Nitroxides: Applications in Chemistry, Biomedicine, and Materials Science, WILEY-VCH Verlag GmbH & Co. KGaA, Weinheim, 2008. ISBN:978-3-527-31889-6.
[26] I. Dozov, N. Kirov, B. Petroff, Phys. Rev. A 36 (5) (1987) 2870.
[27] G.A. Korn, T.M. Korn, Mathematical Handbook for Scientists and Engineers, McGraw-Hill Book Company, New York, 1968.
[28] C.D. Southern, P.D. Brimicombe, S.D. Siemianowski, S. Jaradat, N. Roberts, EPL 82 (2008) 56001.
[29] A. Bobrovsky, V. Shibaev, G. Elyashevitch, E. Rosova, A. Shimkin, V. Shirinyan, A. Bubnov, M. Kaspar, V. Hamplova, M. Glogarova, Liquid Cryst. 35 (5) (2008) 533.

[30] A. Bobrovsky, V. Shibaev, G. Elyashevich, E. Rosova, A. Shimkin, V. Shirinyan, K.-L. Cheng, Polym. Adv. Technol. 21 (2010) 100.
[31] A.V. Fiacco, C.P. McCormick, Nonlinear Programming: Sequential Unconstrained Minimization Techniques, John Wiley and Sons Inc., New York-London-Sydney-Toronto, 1968.
[32] S. Nakatsuji, M. Fujino, S. Hasegawa, J. Org. Chem. 72 (2007) 2021.
[33] S. Nakatsuji, H. Ikemoto, J. Yamada, A. Mor, J. Org. Chem. 68 (2003) 1708.
[34] N. Ikuma, R. Tamura, S. Shimono, Y. Uchida, K. Masaki, J. Yamauchi, Y. Aoki, H. Nohira, Adv. Mater. 18 (2006) 477.
[35] K. Skarp, S.T. Lagewall, B. Stebler, Mol. Cryst. Liquid Cryst. 60 (3) (1980) 215.
[36] G. Elyashevich, A. Kozlov, I. Moneva, Polymer Sci. Series B 40 (1998) 71–74 [Vysokomol. Soyed., 40 (1998) 483–486, in Russian].
[37] J.E. Dennis, D.M. Gay, R.E. Welseh, ACM Trans. Math. Softw. 7 (3) (1981) 348.
[38] G.A.F. Seber, C.J. Wild, Nonlinear Regression, Wiley, New York, 1989.
[39] S.P. Van, G.B. Birrell, O.H. Griffith, J. Magn. Reson. 15 (1974) 444–469.
[40] O.H. Griffith, P. Jost, Lipid spin labels in biological membranes, in: L.J. Berliner (Ed.), Spin Labeling: Theory and applications, Academic Press, New York, 1976, pp. 53–132.

Please cite this article in press as: A.Kh. Vorobiev et al., Chem. Phys. (2012), http://dx.doi.org/10.1016/j.chemphys.2012.10.006